Materials Transactions, Vol. 44, No. 4 (2003) pp. 669 to 672

Magnetic Domain of $Fe_{73.5}Cu_1Nb_3Si_{13.5}B_9$ Studied by Electron Holography Coupled with Thickness Mapping Method*

Yoshitaka Aoyama[1], Young-Gil Park[1], Daisuke Shindo[1] and Yoshihito Yoshizawa[2]

[1]*Institute of Multidisciplinary Research for Advanced Materials, Tohoku University, Sendai 980-8577, Japan*
[2]*Advanced Electronics Research Laboratory, Hitachi Metals, Ltd., Kumagaya 360-0843, Japan*

Magnetic flux in soft magnetic alloy $Fe_{73.5}Cu_1Nb_3Si_{13.5}B_9$ was investigated by electron holography coupled with a thickness mapping method. First the reconstructed phase image of a soft magnetic material with a simple wedge shape was simulated, and the contribution of both magnetic flux and inner potential to the reconstructed phase image was estimated. In the experiment, the magnetic flux was evaluated by removing the effect of inner potential with thickness mapping. The magnetic flux density of $Fe_{73.5}Cu_1Nb_3Si_{13.5}B_9$ obtained was 1.21 T which agreed well with that of a bulk specimen (1.28 T).

(Received November 29, 2002; Accepted February 18, 2003)

Keywords: *electron holography, electron energy loss-spectroscopy, thickness mapping, inner potential, magnetic flux*

1. Introduction

Since transmission electron microscopes with a field emission gun have been developed, electron holography technique[1–4] is now expected to apply widely for characterizing a variety of materials. Electron holography is a unique technique especially for observing the magnetic field in various magnetic materials. The magnetic field can be recorded by the phase shift (ϕ) against periodic interference fringes on an electron hologram. The phase shift can be obtained by using optical process or digital analysis with the Fourier transform. In the reconstructed phase image represented by $\cos(\phi)$, the magnetic field can be imaged with black and white bands corresponding to the lines of magnetic flux. Actually, closure domains have been clearly visualized in soft magnetic material $Fe_{73.5}Cu_1Nb_3Si_{13.5}B_9$.[5)]

On the other hand, it is well known that reconstructed phase images have the effect of not only magnetic flux but also inner potential. Thus, in order to analyze the internal magnetic flux of magnetic materials accurately, it is necessary to remove the effect of inner potential from reconstructed phase images. In this paper, the effect of inner potential is estimated by a thickness mapping method with electron energy-loss spectroscopy (EELS). The distribution and density of the magnetic flux in $Fe_{73.5}Cu_1Nb_3Si_{13.5}B_9$ shown in the reconstructed phase images was analyzed by electron holography taking into account specimen thickness evaluated by EELS.

2. Experimental Procedures

Amorphous $Fe_{73.5}Cu_1Nb_3Si_{13.5}B_9$ alloys were prepared by the single-roller method. The width and thickness of the alloys are 5 mm and 20 μm, respectively. Thin foils for transmission electron microscopy studies were made from ribbon fragments by thinning with low-energy (3.0 keV) Ar ion beam at a 15° inclination.

Electron holography was carried out with a JEM-3000F transmission electron microscope (TEM) with an accelerating voltage of 300 kV. The microscope is equipped with a thermal field-emission gun and a biprism. The biprism and two earth potential electrodes are positioned between objective lens and intermediate lens. In this study, the magnification of image was set to be 4000 times and the voltage of the biprism was set to be 33 V. Electron holograms recorded on conventional EM films were digitalized using a Nikon-LS-3510AF film scanner with resolution of 8 μm/pixel. Reconstructed phase images were obtained from the digitized holograms with the Fourier transform. The phase shift $\phi(x, y)$ due to magnetic flux and inner potential of $Fe_{73.5}Cu_1Nb_3Si_{13.5}B_9$ is represented by $\cos\phi(x, y)$ in the reconstructed phase images. Thus, black and white bands appear alternatively with the increase of the phase shift $\phi(x, y)$.

Thickness mapping was also carried out with a JEM-3000F TEM with a Gatan Imageing Filter (GIF) system. Thickness mapping images were recorded with the slow-scan CCD camera.

3. Results and Discussion

In order to understand the general feature of the reconstructed phase images observed in thin films of soft magnetic materials,[5)] we first carried out the simulation of the reconstructed phase image. Figure 1(a) is a simple model of a magnetic specimen with a wedge shape. The saturation magnetization is assumed to be 1.28 T which corresponds to that of $Fe_{73.5}Cu_1Nb_3Si_{13.5}B_9$ at room temperature, and the orientation of the magnetization is set to be parallel to the specimen edge taking into account van den Berg's effect.[6)] We neglected the effect of the stray field. The reconstructed phase images (b) and (c) are obtained by taking into account the effects of inner potential and magnetic flux, respectively, while the image (d) is obtained with both effects. The feature that the black and white bands appear alternately being parallel to the specimen edge with higher density for thicker region is consistent with the previous observation in $Fe_{73.5}Cu_1Nb_3Si_{13.5}B_9$.[5)] From the simulation in Fig. 1, it is

*This Paper was Presented at the Autumn Meeting of the Japan Institute of Metals, held in Osaka, on November 4, 2002.

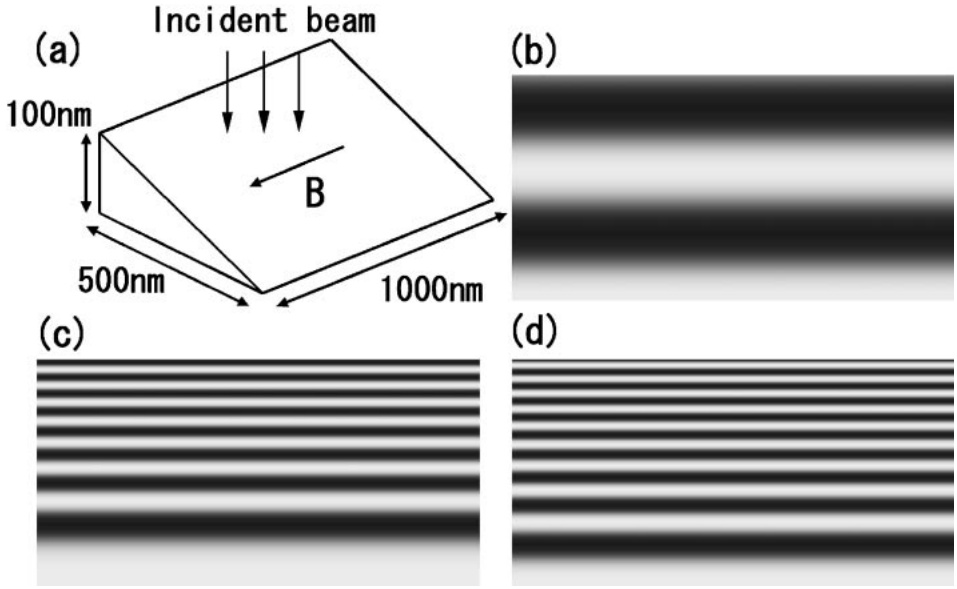

Fig. 1 (a) A wedge-shaped magnetic specimen assumed for simulation. (b) Reconstructed phase image simulated taking into account the inner potential only. (c) Reconstructed phase image simulated taking into account the magnetic flux only. (d) Reconstructed phase image simulated taking into account both the magnetic flux and the inner potential.

found that the effect of inner potential (b) was estimated to be about 16.7% of the phase shift in the reconstructed phase image (d).

Figures 2(a) and (b) show a hologram and a thickness mapping image of $Fe_{73.5}Cu_1Nb_3Si_{13.5}B_9$ prepared by the single-roller method, respectively. In EELS, the intensity of the plasmon peaks increases with the increase of specimen thickness, while the zero-loss intensity decreases with the increase of thickness being complementary to the plasmon peak intensity. In general, a specimen of thickness $t(x, y)$ at the position x, y is given with the total electron intensity $I_t(x, y)$ and the intensity of the zero-loss peak $I_0(x, y)$ as

$$t(x, y) = \lambda_p \ln\left(\frac{I_t(x, y)}{I_0(x, y)}\right) \tag{1}$$

where λ_p is a constant being called the mean free path for inelastic scattering. In the above equation, $I_t(x, y)$ and $I_0(x, y)$ can easily be evaluated from the spectrum, and so the specimen thickness can be determined with high accuracy if λ_p is known. Eventually, the phase shift due to inner potential is given with $t(x, y)$ in (1) as

$$\phi(x, y) = \frac{2\pi e U t(x, y)}{\lambda E} \frac{(E_0 + E)}{(2E_0 + E)} \tag{2}$$

where λ is a wavelength of incident electron beam, and U is the inner potential. λ_p and U are assumed to be the same as those of iron in the analysis below, *i.e.* 210 nm and 15 V, respectively. Also, E and E_0 are the incident electron energy and the electron rest mass energy, respectively. In the thickness mapping image of Fig. 2(b), a relatively bright region is seen in the specimen edge. The region is considered to be the folded region.

Figure 2(c) shows a reconstructed phase image of $Fe_{73.5}Cu_1Nb_3Si_{13.5}B_9$ obtained from Fig. 2(a) with the Fourier transform.[2)] Taking into account the effect of inner potential using eq. (2), the distribution of magnetic flux was

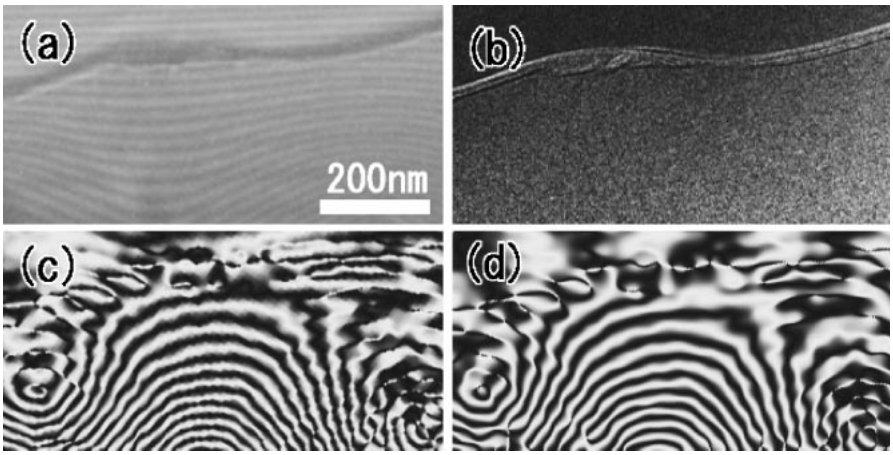

Fig. 2 (a) Electron hologram of $Fe_{73.5}Cu_1Nb_3Si_{13.5}B_9$. (b) Relative thickness mapping image. (c) Reconstructed phase image containing the effects of both magnetic flux and inner potential. (d) Reconstructed phase image obtained by removing the effect of inner potential.

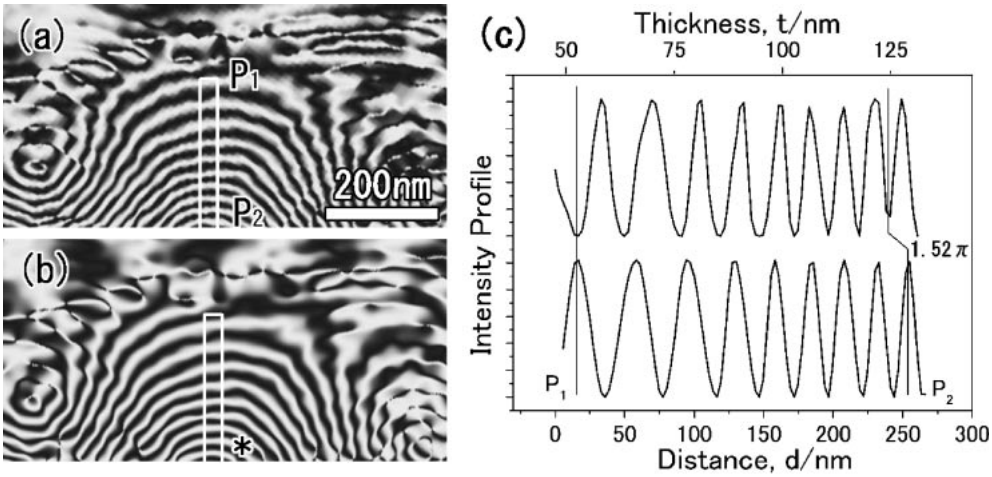

Fig. 3 (a) Reconstructed phase image of $Fe_{73.5}Cu_1Nb_3Si_{13.5}B_9$. (b) Reconstructed phase image obtained by removing the effect of inner potential. (c) Intensity profiles of the reconstructed phase images (a,b) from P_1 to P_2. Horizontal axes at the top and bottom indicate specimen thickness and the distance from P_1.

obtained as shown in Fig. 2(d). It is seen that the interval of the white bands in Fig. 2(d) is wider than that of Fig. 2(c). The feature in the reconstructed phase images of Figs. 2(c) and (d) correspond well to those of Figs. 1(d) and (c). It should be noted that the phase shift of the electron is generally given as

$$\phi = \frac{e}{\hbar}\oint(\varphi dt - \bar{A}d\bar{r}) \tag{3}$$

where φ is electric potential, $\bar{A}$ is the vector potential.[1,2] In eq. (3), since the second term is given with the vector, the sign of phase shift ϕ depends on the direction of the vector potential or magnetic flux.[2] Thus if the direction of magnetization is opposite, the interval of the white bands in the reconstructed phase images becomes narrow. Figure 3 shows the detailed intensity profiles of Figs. 2(c) and (d). Since there exists some irregularity at the specimen surface, the irregularity and the folded region affect the evaluation of inner potential and magnetic flux much at the thin specimen region. Thus we estimated the magnetic flux at the relatively thick region in Fig. 3. At the ninth peaks as indicated by arrows, for example, there is the phase difference of 1.52 π, which corresponds to the effect of inner potential being 19.0% to the total phase shift. It is known that the relation between magnetic flux density B and the distance of white bands l is given as[2]

$$l = \frac{h}{etB} \tag{4}$$

Taking into account the specimen thickness evaluated by EELS, it is found that the magnetic flux density at the point (*) in Fig. 3(b) is evaluated to be about 1.21 T which is consistent with the magnetic flux 1.28 T of the bulk $Fe_{73.5}Cu_1Nb_3Si_{13.5}B_9$. It can be said that the combination of electron holography and a thickness mapping method with EELS is promising to evaluate the magnetic flux accurately, and expected to apply to magnetization analysis of various advanced magnetic materials.

4. Conclusions

From the analysis of electron holography and thickness mapping with EELS on a $Fe_{73.5}Cu_1Nb_3Si_{13.5}B_9$ alloy, following results are obtained

(1) Simulation of the reconstructed phase image of a soft magnetic material with a wedge shape is carried out taking into account the effects of both magnetic flux and inner potential. The general feature of the distribution and density change in white bands in the reconstructed phase image reproduce well those of the reconstructed phase images experimentally obtained.
(2) Magnetic flux was evaluated quantitatively by subtracting the effect of inner potential estimated by the thickness mapping method with EELS from the reconstructed phase image.
(3) The magnetic flux density (1.21 T) of $Fe_{73.5}Cu_1Nb_3Si_{13.5}B_9$ obtained taking into account the specimen thickness is found to be consistent with that of the bulk specimen (1.28 T).

Acknowledgements

This work was supported by Grant-in-Aid for Scientific Research (B) from Japan Society for the Promotion of Science, and by the Special Coordination Funds for Promoting Science and Technology on ''Nanohetero Metallic Materials'' from the Science and Technology Agency.

REFERENCES

1) A. Tonomura: *Electron Holography*, Second Edition, (Springer-Verlag Berlin, 1999).
2) D. Shindo and T. Oikawa: *Analytical Electron Microscopy for Materials Science*, (Springer-Verlag Tokyo, 2002) pp. 116–125.
3) T. Hirayama, G. Lai, T. Tanji, N. Tanaka and A. Tonomura: J. Appl. Phys. **82** (1997) 522–527.
4) Y. Aoyama, Y.-G. Park, C. W. Lee and D. Shindo: Mater. Trans. **42** (2001) 474–477.
5) D. Shindo, Y.-G. Park and Y. Yoshizawa: J. Magn. Magn. Mater. **238** (2002) 101–108.

6) *Alex Hubert and Rudolf Schäfer: Magnetic Domains*, (Springer-Verlab Berlin Heidelberg, 1998) pp. 169–173.
7) S. Frabboni, G. Matteucci, G. Pozzi and M. Vanzi: Phys. Rev. Lett. **55** (1985) 2196–2199.
8) J. W. Chen, G. Matteucci, A. Migliori, G. F. Missiroli, E. Nichelatti, G. Pozzi and M. Vanzi: Phys. Rev. A **40** (1989) 3136–3146.
9) T. Hirayama, J. Chen, Q. Ru, K. Ishizuka, T. Tanji and A. Tonomura: J. Electron Microsc. **43** (1994) 190–197.
10) Y.-G. Park, D. Shindo and M. Okada: Mater. Trans., JIM **41** (2000) 1132–1135.